Real-time parameter estimation of nonlinear vessel steering model using support vector machine

Haitong Xu
Centre for Marine Technology and Ocean Engineering (CENTEC), Instituto Superior Técnico, Universidade de Lisboa.
Av. Rovisco Pais, Lisboa 1049-001, Portugal;
e-mail: haitong.xu@centec.tecnico.ulisboa.pt

M.A. Hinostroza
Centre for Marine Technology and Ocean Engineering (CENTEC), Instituto Superior Técnico, Universidade de Lisboa.
Av. Rovisco Pais, Lisboa 1049-001, Portugal;
e-mail: miguel.hinostroza@centec.tecnico.ulisboa.pt

Vahid Hassani
Department of Marine Technology, Norwegian University of Science and Technology, 7491 Trondheim, Norway.
Department of Ships and Ocean Structures, SINTEF Ocean, Trondheim, Norway.
e-mail: vahid.hassani@ntnu.no

C. Guedes Soares [1]
Centre for Marine Technology and Ocean Engineering (CENTEC), Instituto Superior Técnico, Universidade de Lisboa.
Av. Rovisco Pais, Lisboa 1049-001, Portugal;
e-mail: c.guedes.soares@centec.tecnico.ulisboa.pt
Fellow ASME

ABSTRACT

The least-square support vector machine (LS-SVM) is used to estimate the dynamic parameters of a nonlinear marine vessel steering model in real-time. First, manoeuvring tests are carried out based on a scaled free-running ship model. The parameters are estimated using standard LS-SVM and compared with the theoretical solutions. Then, an online version, a sequential least square support vector machine, is

[1] Corresponding author

derived and used to estimate the parameters of vessel steering in real-time. The results are compared with the values estimated by standard LS-SVM with batched training data. By comparison, sequential least square support vector machine can dynamically estimate the parameters successfully, and it can be used for designing a dynamic model-based controller of marine vessels.

INTRODUCTION

Mathematical models of marine vehicles are playing a more important role in marine control with the development of numerical computation. Linear Nomoto model is widely used for heading control, but due to its over-simplified structure [1], the Nomoto model with fixed parameters usually cannot provide an accurate prediction of heading response due to the environmental disturbances. A model with dynamic parameters is a good option and is now drawing more attention [2]. A steering model with dynamic parameters can provide a more accurate response compared with the static model, and it is more capable of dealing with the dynamic environment disturbance due to waves, wind and current.

System identification has been used to improve and validate models with data from either free-model or full-scale tests [3]. Various techniques have been proposed for mathematical modelling of marine vessels. For example, in [4], a neural network was used to identify the nonlinear and coupled damping for an underwater vehicle. In [5], the nonlinear viscous damping forces in the horizontal plane of a surface vessel at low speed was estimated using the least square method. The least squares method is a very classic technique for system identification. It was used to estimate the hydrodynamic coefficients based on Planar Motion Mechanism (PMM) tests by Ross *et al.*[6], and Hassani *et. al.* [7], but it usually will drop into local optimum and is largely affected by the noise of training data [8]. In [9–11], the least square method was used to estimate the parameters of a nonlinear manoeuvring mathematical model, and a classic genetic algorithm, which is an intelligent algorithm for solving both constrained and unconstrained optimization problems [12], was used to search the global optimum of a cost function using free-running model test data. In [13], a regularized least-squares method was used to solve the hyper-parameter estimation problem with large data sets and ill-conditioned computations. Truncated singular value decomposition (TSVD) [14,15] is also a popular method to solve the ill-conditioned problem of least square method, and its application for parameters estimation of ship manoeuvring model was presented in [16].

Extended Kalman filter (EKF) is an optimal recursive estimator, so it can update the unknown variables in real-time when new measurements arrive. In [2,17], the extended Kalman filter was used to estimate the dynamic parameters of a modified Nomoto model for vessel steering. Fossen *et al.* discussed an off-line parallel extended Kalman filter (EKF) algorithm utilizing two measurement series in parallel to estimate the parameters in the DP ship model [18]. In [19], the maximum likelihood method was used to determine ship steering dynamics.

Recently, support vector machine (SVM) was applied to estimate the hydrodynamic coefficients of ship model [20,21]. SVM is a universal learning machine in the framework of structural risk minimization (SRM) [22]. In [23,24], a modified version, Least Squares Support Vector Machines, was applied to model the controller of the marine surface vehicle for path following scenarios based on the manoeuvring tests. In order to estimate the parameters in real- time, an incremental update algorithm for training SVM online was proposed by Cauwenberghs et al. [25]. A nonlinear generalized predictive controller based on online LS-SVM was presented in [26]. Tang et al. [27] used an online sequential weighted LS-SVM to identify the structural parameters and their changes.

The main result of this paper is the implementation of online parameter estimations of nonlinear vessel steering model based on LS-SVM. Firstly, a nonlinear 2nd order Nomoto model for ship steering is briefly introduced and manoeuvring tests recommended by ITTC [28] have been carried out based on a scaled free-running ship model. The standard LS-SVM is introduced and used to estimate the parameters of the vessel steering model using batched training data. The effectiveness of parameters estimation based on standard LS-SVM is demonstrated by comparison with the theoretical solution.

Then, a sequential LS-SVM is derived based on the incremental updating algorithm. It is different from the online SVM using dynamic windows, which usually train the model using the truncated data. Sequential LS-SVM can estimate the parameters dynamically with the arrival of a new measurement. Parameters are updated in an incremental way, which avoids expensive inversion operation for training the model. Last, sequential LS-SVM is used to estimate the parameters of the nonlinear Nomoto model with the free-running test data.

This paper is organized as follows: Section 2 is a brief introduction of the nonlinear model for ship steering. Section 3 offers a detail description of the principle of standard LS-SVM and sequential LS-SVM based on incremental updating algorithm. In section 4, free-running model test is presented using a scaled ship model. In section 5, the validation of parameter estimation using standard LS-SVM is presented and sequential LS-SVM is used to estimate the parameters in real-time. The conclusions are presented in Section 6.

NONLINEAR MATHEMATICAL MODEL FOR SHIP STEERING

The Abkowitz model [29] is widely used to describe the ship dynamic motion. It is obtained using Newton's laws, and the hydrodynamic forces are approximated using Taylor expansions. In order to simplify the control problem, surge speed can be assumed as a constant value, so the equation of surge motion can be decoupled from the other two and plays no further part in any linear treatment of ship steering. The linear expansions of sway and yaw motion equations can be expressed:

$$\begin{aligned}(m-Y_{\dot v})\dot v+(mx_G-Y_{\dot r})\dot r+mur&=Y_v v+Y_r r+Y_\delta\delta\\(mx_G-N_{\dot v})\dot v+(I_Z-N_{\dot r})\dot r+mx_G ur&=N_v v+N_r r+N_\delta\delta\end{aligned}\quad(1)$$

By eliminating the equation of sway motion in Eq.1, the resulted equation is the 2nd order linear equation of yaw motion, which is well known as the 2nd-order Nomoto model [30].

$$T_1T_2\ddot r+(T_1+T_2)\dot r+r=K_\delta(\delta_R+T_3\dot\delta_R)\quad(2)$$

The yaw rate equation is widely used to describe the course keeping behaviour of a ship and its Laplace Transform version is used in many ship control and autopilot studies [31]. The transfer function of 2nd-order Nomoto model is given as:

$$\frac{r}{-\delta_R}=\frac{K_\delta(1+T_3s)}{(1+T_1s)(1+T_2s)}\quad(3)$$

The 2nd-order linear Nomoto model can be used for the course control but its accuracy for the prediction of the yaw rate is not adequate due to the over-simplified structure [32]. Therefore, the nonlinear Nomoto model can be obtained by including the nonlinear term in Eq.2

$$T_1T_2\ddot r+(T_1+T_2)\dot r+ar^3+r=K_\delta(\delta_R+T_3\dot\delta_R)\quad(4)$$

where *a* is the coefficient of the nonlinear term. In Eq.3, the pole term $(1+T_2 s)$ and the zero terms $(1+T_3 s)$ nearly cancel each other [19,33], because the difference between T_2 and T_3 is small, they are usually of the same order of magnitude. Therefore, the pole-zero cancellation can be implied to simplify this equation. The resulted equation is the well-known 1st-order Nomoto model.

$$T\dot{r} + r = K_\delta \delta_R \quad (5)$$

LS-SVM FOR PARAMETER ESTIMATION

In this section, the standard LS-SVM [34] will be introduced briefly and an extended version, the sequential LS-SVM based on incremental updating algorithm, is also derived. The sequential LS-SVM can update the estimated parameters in real-time when new data added to the training set.

Standard LS-SVM for parameter estimation

Firstly considering the training set, $\boldsymbol{S} = \{s_i \mid s_i = (x_i, y_i), x_i \in \Re^n, y_i \in \Re\}_{i=1}^N$, where x_i is the input and y_i is the output. For regression purposes, Support Vector Regression (SVR) gives a general approximation function form:

$$y(x) = \boldsymbol{w}^T \boldsymbol{\varphi}(x) + b \quad (6)$$

where *x* is the training sample; *y(x)* is the target value; *b* is the bias term; ***w*** is a weight matrix; $\boldsymbol{\varphi}(x)$ is kernel function, which is used to map the training sample to a higher dimensional feature space. For parameter estimation purpose using LS-SVM, the following optimization problem is formulated:

$$\begin{aligned} \min_{w,b,e_i} \quad & f(w,e) = \frac{1}{2}\boldsymbol{w}^T\boldsymbol{w} + \frac{1}{2}C\sum_{i=1}^N e_i^2 \\ s.t. \quad & y_i = \boldsymbol{w}^T\boldsymbol{\varphi}(x_i) + b + e_i \end{aligned} \quad (7)$$

where $e_i, i = 1 \cdots N$, is the error, and *C* is the regularization factor. As presented in Eq.7, the minimization of $\boldsymbol{w}^T \boldsymbol{w}$ is closely related to the use of a weight decay term in the training of neural networks, and the $\sum_{i=1}^{N} e_i^2$ is the empirical error. Therefore, the regularization factor, *C* balances the model accuracy and the model complexity, which also known as structural risk.

The corresponding Lagrange function is given by:

$$\mathcal{L}(\boldsymbol{w}, b, e_i, \alpha_i) = \frac{1}{2}\boldsymbol{w}^T \boldsymbol{w} + \frac{1}{2} C \sum_{i=1}^{N} e_i^2 - \sum_{i=1}^{N} \alpha_i [\boldsymbol{w}^T \boldsymbol{\varphi}(x_i) + b + e_i - y_i] \quad (8)$$

where α_i are the Lagrange multipliers. The optimality condition, Karush-Kuhn-Tucker conditions (KKT) [34,35], are defined by computing the derivative of Eq.8 with respect to $\boldsymbol{w}, b, e_i, \alpha_i$:

$$\begin{aligned}
&\frac{\partial \mathcal{L}}{\partial \boldsymbol{w}} = 0 \quad \rightarrow \quad \boldsymbol{w} = \sum_{i=1}^{N} \alpha_i \boldsymbol{\varphi}(x_i) \\
&\frac{\partial \mathcal{L}}{\partial b} = 0 \quad \rightarrow \quad \sum_{i=1}^{N} \alpha_i = 0 \\
&\frac{\partial \mathcal{L}}{\partial e_i} = 0 \quad \rightarrow \quad \alpha_i = C e_i \\
&\frac{\partial \mathcal{L}}{\partial \alpha_i} = 0 \quad \rightarrow \quad \boldsymbol{w}^T \boldsymbol{\varphi}(x_i) + b + e_i - y_i = 0
\end{aligned} \quad (9)$$

where $i = 1 \cdots N$. Eliminating variables $\boldsymbol{w}$ and e_i and rewriting Eq.9 in matrix representation.

$$\underbrace{\begin{bmatrix} 0 & \vec{\boldsymbol{1}} \\ \vec{\boldsymbol{1}} & K(\cdot) + C^{-1}\boldsymbol{I} \end{bmatrix}}_{\boldsymbol{A}_N} \underbrace{\begin{bmatrix} b \\ \vec{\alpha} \end{bmatrix}}_{\boldsymbol{\theta}_N} = \underbrace{\begin{bmatrix} 0 \\ \vec{Y} \end{bmatrix}}_{\boldsymbol{Y}_N} \quad (10)$$

where $\vec{\boldsymbol{1}}$ is a unit array, $\vec{\boldsymbol{1}} = [1, 1, \cdots, 1]_{1 \times N}$. $\boldsymbol{I}$ is an $N \times N$ identity matrix, $\vec{\alpha} = [\alpha_1, \cdots \alpha_N]^T$, $\vec{Y} = [y_1, \cdots, y_N]^T$. $K(x_k \cdot x_i) = \varphi(x_k)^T \varphi(x_i), i, k = 1, 2, \cdots N$ is the kernel function that represents an inner product between its operands. It is positive definite and satisfies the Mercer condition [35,36]. In this paper, the linear kernel function is used for parameter identification. LS-SVM model for function estimation follows:

$$y(x) = \sum_{i=1}^{N} \alpha_i K(x \cdot x_i) + b \quad (11)$$

Sequential LS-SVM

Based on the above discussion, assume the LS-SVM has been trained using the first N pairs of data, and a new data pair (x_{N+1}, y_{N+1}) is observed. As presented in Eq.10, when a new data added to the training set, LS-SVM can be written as:

$$\boldsymbol{A}_{N+1}\boldsymbol{\theta}_{N+1} = \boldsymbol{Y}_{N+1} \quad \rightarrow \quad \boldsymbol{\theta}_{N+1} = \boldsymbol{A}_{N+1}^{-1}\boldsymbol{Y}_{N+1} \quad (12)$$

where

$$\boldsymbol{A}_{N+1} = \begin{bmatrix} \boldsymbol{A}_N & \boldsymbol{b} \\ \boldsymbol{b}^T & c \end{bmatrix} \quad (13)$$

$$\boldsymbol{b} = \left[1, k_{1,N+1}, k_{2,N+1}, \cdots, k_{N,N+1}\right]^T \quad (14)$$

$$c = C^{-1} + k_{N+1,N+1} \quad (15)$$

$$\boldsymbol{Y}_{N+1} = \begin{bmatrix} \boldsymbol{Y}_N \\ y_{N+1} \end{bmatrix} \quad (16)$$

where $k_{i,j}$ is the element of the kernel matrix. Now, in order to get the new parameters matrix, $\boldsymbol{\theta}_{N+1}$, the problem is how to find the solution of the matrix $\boldsymbol{A}_{N+1}$. In batched LS-SVM, matrix inversion is calculated directly. But for real-time parameter estimated, computing of the matrix inverse is impractical, because it is usually time-consuming and needs a lot of memory when handling large sets of data. In the following part, an incremental updating algorithm will be presented for calculation of the inverse of the matrix $\boldsymbol{A}_{N+1}$. Two lemmas need to be given first. As presented in [37]:

Lemma 1. *The matrix $\boldsymbol{A}$ is invertible if $\boldsymbol{A}_{11}^{-1}$ and $\boldsymbol{A}_{22}^{-1}$ exist, and the inverse matrix, $\boldsymbol{A}^{-1}$ is given as:*

$$\boldsymbol{A}=\begin{bmatrix}\boldsymbol{A}_{11} & \boldsymbol{A}_{12}\\ \boldsymbol{A}_{21} & \boldsymbol{A}_{22}\end{bmatrix} \tag{17}$$

$$\boldsymbol{A}^{-1}=\begin{bmatrix}\left[\boldsymbol{A}_{11}-\boldsymbol{A}_{12}\boldsymbol{A}_{22}^{-1}\boldsymbol{A}_{21}\right]^{-1} & \boldsymbol{A}_{11}^{-1}\boldsymbol{A}_{12}\left[\boldsymbol{A}_{21}\boldsymbol{A}_{22}^{-1}\boldsymbol{A}_{12}^{-1}-\boldsymbol{A}_{22}\right]^{-1}\\ \left[\boldsymbol{A}_{21}\boldsymbol{A}_{11}^{-1}\boldsymbol{A}_{12}-\boldsymbol{A}_{22}\right]^{-1}\boldsymbol{A}_{21}\boldsymbol{A}_{11}^{-1} & \left[\boldsymbol{A}_{22}-\boldsymbol{A}_{21}^{-1}\boldsymbol{A}_{11}^{-1}\boldsymbol{A}_{12}\right]^{-1}\end{bmatrix} \tag{18}$$

Lemma 2. If $\boldsymbol{A}^{-1}$, $\boldsymbol{E}^{-1}$ *exist, then the following equation is true:*

$$(\boldsymbol{A}+\boldsymbol{BEF})^{-1}=\boldsymbol{A}^{-1}-\boldsymbol{A}^{-1}\boldsymbol{B}(\boldsymbol{E}^{-1}+\boldsymbol{FA}^{-1}\boldsymbol{B})^{-1}\boldsymbol{FA}^{-1} \tag{19}$$

where matrices $\boldsymbol{A}\in R^{n\times n},\boldsymbol{B}\in R^{n\times m},\boldsymbol{E}\in R^{m\times m},\boldsymbol{F}\in R^{m\times n}$.

According to the *Lemma 1* and *Lemma 2*, obviously, the inverse matrix of $\boldsymbol{A}_N$ and c exist. Therefore, the inverse matrix $\boldsymbol{A}_{N+1}^{-1}$ is given:

$$\boldsymbol{A}_{N+1}^{-1}=\begin{bmatrix}\boldsymbol{A}_N & \boldsymbol{b}\\ \boldsymbol{b}^T & c\end{bmatrix}^{-1}=\begin{bmatrix}\left[\boldsymbol{A}_N-\frac{1}{c}\boldsymbol{bb}^T\right]^{-1} & \boldsymbol{A}_N^{-1}\boldsymbol{b}\left[\boldsymbol{b}^T\boldsymbol{A}_N^{-1}\boldsymbol{b}-c\right]^{-1}\\ \left[\boldsymbol{b}^T\boldsymbol{A}_N^{-1}\boldsymbol{b}-c\right]^{-1}\boldsymbol{bA}_N^{-1} & \left[c-\boldsymbol{b}^T\boldsymbol{A}_N^{-1}\boldsymbol{b}\right]^{-1}\end{bmatrix} \tag{20}$$

in which, the top left submatrix in Eq.20 can be rewritten as:

$$\left[\boldsymbol{A}_N-\frac{1}{c}\boldsymbol{bb}^T\right]^{-1}=\boldsymbol{A}_N^{-1}+\boldsymbol{A}_N^{-1}\boldsymbol{b}\left[c-\boldsymbol{b}^T\boldsymbol{A}_N^{-1}\boldsymbol{b}\right]\boldsymbol{b}^T\boldsymbol{A}_N^{-1} \tag{21}$$

Denoting, $\Delta=\left[c-\boldsymbol{b}^T\boldsymbol{A}_N^{-1}\boldsymbol{b}\right]^{-1}$, then Eq.20 can be rewritten in matrix expression:

$$\boldsymbol{A}_{N+1}^{-1}=\begin{bmatrix}\boldsymbol{A}_N^{-1} & \vec{0}\\ \vec{0} & 0\end{bmatrix}+\Delta\begin{bmatrix}\boldsymbol{A}_N^{-1}\boldsymbol{b}\\ -1\end{bmatrix}\begin{bmatrix}\boldsymbol{b}^T\boldsymbol{A}_N^{-1} & -1\end{bmatrix} \tag{22}$$

With Eq.22, the inverse matrix of $\boldsymbol{A}_N$ is computed in an incremental way, which avoids expensive inversion operation. The parameter matrix can be updated with the new data added to the training set. Therefore, the real-time parameters estimation can be implemented with Eq.22.

FREE-RUNNING MODEL TESTS

In this section, the results of manoeuvring tests onboard a self-running ship model are presented. The self-propelled vehicle is a scaled ship model of a chemical tanker, and the total length is 2.58 meters. On the ship, various sensors have been installed. The tests were conducted in an outdoor pool with moderate wind conditions.

Ship model dimensions and hardware structure

The self-propelled vehicle is presented in Fig.1. The model is constructed from single skin glass reinforced polyester, with plywood framing and its design speed is 0.98 m/s. Its main particularities are given in Table 1.

Fig. 1
Table 1

The self-running ship model is equipped with several sensors and actuators, i.e. 6-DOF fibre-optic gyrocompass, differential GPS, DC motor, industrial WI-FI communication, Compact-RIO embedded acquisition system, and batteries. The equipment is controlled and synchronized using LABVIEW 2013 software, based on a real-time acquisition program. The hardware structure is presented as in Fig.2. The software architecture consists of several program loops: FPGA loop, real-time loop and TCP/IP loop [38,39].

Free-running model test results

Free-running model tests on the scaled model were conducted during the period of March 2016 to May 2016 at swimming pool of "Piscina Oceânica", Oeiras, Portugal. The weather was sunny and dry, but some wind was constantly present, changing its speed (approximately in the interval of 1–3 m/s) and direction as time passed. The pool is deep enough to neglect any shallow-water effects. The pool has a maximum length of 50 m and an average breadth of 20 m.

Fig.2

The model was carefully launched in water and partly ballasted to get zero list and trim, although the design draught was not reached in these tests. Also, the model was not calibrated in the sense of reaching the scaled vertical position of the centre of gravity and scaled values of the moments of inertia. During all manoeuvres, the rpm was kept constant. The $20^\circ-20^\circ$ zigzag manoeuvring tests [28] have been carried out and the results are presented in Fig.3-4. Fig.3 shows that the collected data have a high quality and is suitable to carry out further manoeuvrability analysis of the scaled ship model. In Fig.4, the wind speed is about 2 m/s and the direction are changing rage from $80^\circ-100^\circ$.

Fig. 3

Fig. 4

REAL-TIME PARAMETERS ESTIMATION AND VALIDATION

In this section, the standard LS-SVM is used to estimate the parameters of the 1st-order Nomoto model using batched training data. The validation is presented by comparing the obtained parameters with theoretical solutions, which are calculated directly using $20^\circ-20^\circ$ zigzag manoeuvring test. Then, the sequential LS-SVM is used to estimate the parameters of the nonlinear 2nd order Nomoto model in real-time, and the obtained parameters are compared with the results of standard LS-SVM.

Validation of standard LS-SVM

In order to validate the effectiveness of standard LS-SVM, the analysis method presented in Refs. [40–42] will be used to obtain the parameters. Integrating Eq.8 with respect to time *t*, gives:

$$T\int_0^t \dot{r}dt + \int_0^t rdt = K_\delta \int_0^t \delta_R dt \quad (23)$$

By choosing the range of time, the parameters can be given by the following equations

$$K_\delta = -\frac{\psi_1 - \psi_2}{\int_{t_1}^{t_2} \delta_R dt} \quad (24)$$

$$\frac{K_\delta}{T} = -\frac{r_3 - r_4}{\int_{t_3}^{t_4} \delta_R dt} \quad (25)$$

As shown in Fig.5, the shaded area gives the integral term at points delimited by the cross, where the yaw rate *r* is zero. According to the Eq.24 the parameter K_δ can be found, as $K_\delta = 0.2062$. Similarly, the Eq.25 is applied to the first two zero crossing points of the heading record as shown in the Fig.5. In this case, the heading equal to zero and *T* =2.5221 can be calculated from Eq.25. As presented in Table 2, the difference between estimated and theoretical values is small. Therefore, standard LS-SVM based on batched training data is an effective method and can provide accurate parameters. It will be used to estimate the parameters of the nonlinear 2^{nd}-order Nomoto model in the following part.

Fig. 5

Table 2.

Real-Time parameter estimation using sequential LS-SVM

In this part, $20^\circ - 20^\circ$ and $30^\circ - 30^\circ$ zigzag manoeuvring tests are used as training data. Firstly, the stranded LS-SVM is used to estimate the parameters of the nonlinear 2^{nd} order

Nomoto model. In order to simulate the online situation, the sample in the training set will be fed into the Sequential LS-SVM by time step. Therefore, the dynamic parameters can be obtained and updated with the feedback measurement at each time step. Before the simulation, the number of the initial training set (N) need to be defined. It is used to estimate the initial parameters. In this paper, the size of the initial training set is 10. The Sequential LS-SVM is described in the Algorithm (1).

Algorithms 1.

The standard LS-SVM is used to estimate the parameters of the nonlinear Nomoto model using the batched $20^\circ-20^\circ$ and $30^\circ-30^\circ$ zigzag manoeuvring data. The obtained parameters are given in Table 3. The parameters K_δ has a bit drift from the theoretical value since the nonlinear model is selected. Usually, parameter T can be estimated using the empirical formula (T=T_1+T_2-T_3 = 2.8011 and 2.5049, respectively). It is close to the theoretical value. The values of T2 and T3 are similar, which also indicate that the previous cancellation is reasonable. The obtained Nomoto model is used to predict the response of yaw and yaw rate during the $20^\circ-20^\circ$ and $30^\circ-30^\circ$ zigzag manoeuvring test. The prediction and experimental results are presented in Fig.6, and they are in good agreement. The heading errors in time history is given in Fig. 7. The dynamic estimation of nonlinear parameters using sequential LS-SVM is presented in Fig.8. As shown in Fig. 8a, the parameters are zero at the begin, because initial training set needs to be built first. Then the parameters converge to the values, which are estimated using standard LS-SVM. After 30 seconds, most of the parameters converge to the estimated values, it means that the sequence LS-SVM can find the optimal values with limited samples, which is an advantageous feature compared with the least square method. The least squares method, theoretically, needs infinity training data to find the optimal values, but in most cases, the training data is limited. In Fig. 8b, the parameters, T_1 and K_δ, converges to the estimated values after 20 seconds. For both cases, the coefficient of the nonlinear term does not converge due to the change of the environmental disturbance.

Table 3.
Fig. 6
Fig. 7
Fig. 8

CONCLUSIONS

In this paper, a nonlinear mathematical model for ship steering was briefly described. It is an extended version of the 2nd-order Nomoto model by including nonlinear terms. In order to estimate the parameters, a scaled ship model was built, and a control and measure system was programmed in platform using LABVIEW. Various zigzag tests have been carried out in a swimming pool. Then Standard LS-SVM is introduced briefly and used to estimate the parameters of the manoeuvring model. The obtained parameters agree well with the theoretical values, which validate its effectiveness.

In order to estimate the parameters dynamically, a sequential LS-SVM was derived based on an incremental updating algorithm. Sequential LS-SVM can update the parameters dynamically when new data are fed back into the identification system. It is different from the well-established estimation method based on a dynamic window. For the estimation based on the dynamic window, it can estimate the parameters in real-time, but the model needs to be trained in each time step. For sequential LS-SVM, the parameters are updated in an incremental way, which avoids expensive training operation in each time-step. The parameters obtained by sequential LS-SVM are compared with the values estimated using standard LS-SVM and theoretical values. They are in very good agreement, and the parameters converge to the values with limited training data. Therefore, the proposed method can dynamically update the parameters, which converge to the theoretical values fast, in presence of persistent excitation, and it can be used for designing a dynamic model-based autopilot of marine vessels.

ACKNOWLEDGEMENT

This work was performed within the Strategic Research Plan of the Centre for Marine Technology and Ocean Engineering (CENTEC), which is financed by Portuguese Foundation for Science and Technology (Fundação para a Ciência e Tecnologia-FCT) under contract UID/Multi/00134/2013 - LISBOA-01-0145-FEDER-007629. This work was partly supported by the Research Council of Norway through the Centres of Excellence funding scheme, Project number 223254 – AMOS. This work is a contribution to the project M&MSHIPS - “Maneuvering & Moored SHIPS in ports” (PTDC/EMSTRA/5628/2014) funded by the Portuguese Foundation for Science and Technology. The experiments with the vessel model were not possible without the collaboration of Eng. José Costa, Coordinator of the “Piscina Oceanica”, Oeiras, Portugal, who allowed the realization of the manoeuvring tests in their installations.

NOMENCLATURE

$N_v, N_r, N_\delta, N_{\dot{v}}, N_{\dot{r}}$	Hydrodynamic coefficients of yaw moment
$Y_v, Y_r, Y_\delta, Y_{\dot{v}}, Y_{\dot{r}}$	Hydrodynamic coefficients of sway force
$\boldsymbol{v}$	Generalized velocity in body-fixed frame
δ	Rudder angle
r	Yaw rate
a	The coefficient of the nonlinear term in Nomoto model
T_1, T_2, T_3	Nomoto constant
K_δ	Rudder constant
$\boldsymbol{w}$	Weight matrix
$\boldsymbol{\varphi}(\cdot)$	Kernel function
C	Regularization factor
$\sum_{i=1}^{N} e_i^2$	Empirical error
b	Bias term
$\mathcal{L}(\boldsymbol{w}, b, e_i, \alpha_i)$	Lagrange function
$\boldsymbol{A}_N$	Input matrix
$\boldsymbol{Y}_N$	Output matrix
$\boldsymbol{\theta}_N$	Parameter matrix

REFERENCES

[1] Sutulo, S., Moreira, L., and Guedes Soares, C., 2002, "Mathematical Models for Ship Path Prediction in Manoeuvring Simulation Systems," Ocean Eng., **29**(1), pp. 1–19.

[2] Perera, L. P., Oliveira, P., and Guedes Soares, C., 2015, "System Identification of Nonlinear Vessel Steering," J. Offshore Mech. Arct. Eng., **137**(3), p. 031302.

[3] Revestido Herrero, E. E., and Velasco González, F. J., 2012, "Two-Step Identification of Non-Linear Manoeuvring Models of Marine Vessels," Ocean Eng., **53**, pp. 72–82.

[4] van de Ven, P. W. J., Johansen, T. A., Sørensen, A. J., Flanagan, C., and Toal, D., 2007, "Neural Network Augmented Identification of Underwater Vehicle Models," Control Eng. Pract., **15**(6), pp. 715–725.

[5] Golding, B., Ross, A., and Fossen, T. I., 2006, "Identification of Nonlinear Viscous Damping for Marine Vessels," *14 Th IFAC Symposium on System Identification*, Newcastle , Australia , 2006, pp. 332–337.

[6] Ross, A., Selvik, O., Hassani, V., Ringen, E., and Fathi, D., 2015, "Identification of Nonlinear Manoeuvring Models for Marine Vessels Using Planar Motion Mechanism Tests," *ASME 2015 34th International Conference on Ocean, Offshore and Arctic Engineering*, ASME, Newfoundland, Canada, p. V007T06A014.

[7] Hassani, V., Fathi, D., Ross, A., Sprenger, F., Selvik, Ø., Berg, T. E. T. E., Fathi, D., Sprenger, F., and Berg, T. E. T. E., 2015, "Time Domain Simulation Model for Research Vessel Gunnerus," *ASME 2015 34th International Conference on Ocean, Offshore and Arctic Engineering*, ASME, Newfoundland, Canada, p. V007T06A013.

[8] Söderström, T., 2013, "Comparing Some Classes of Bias-Compensating Least Squares Methods," Automatica, **49**(3), pp. 840–845.

[9] Sutulo, S., and Guedes Soares, C., 2014, "An Algorithm for Offline Identification of Ship Manoeuvring Mathematical Models from Free-Running Tests," Ocean Eng., **79**, pp. 10–25.

[10] Sutulo, S., and Guedes Soares, C., 2015, "Offline System Identification of Ship Manoeuvring Mathematical Models with a Global Optimization Algorithm," *MARSIM 2015*, Newcastle, United Kingdom, pp. 8–11.

[11] Xu, H. T., Hinostroza, M. A., and Guedes Soares, C., 2018, "Estimation of Hydrodynamic Coefficients of a Nonlinear Manoeuvring Mathematical Model with Free-Running Ship Model Tests," Int. J. Marit. Eng., **160**(A3), p. A-213-A-226.

[12] Xu, H. T., and Guedes Soares, C., 2018, "An Optimized Energy-Efficient Path Following Algorithm for Underactuated Marine Surface Ship Model," Int. J. Marit. Eng., **160**(A4), p. A-411-A-421.

[13] Chen, T., and Ljung, L., 2013, "Implementation of Algorithms for Tuning Parameters in Regularized Least Squares Problems in System Identification," Automatica, **49**(7), pp. 2213–2220.

[14] Golub, G. H., and Reinsch, C., 1970, "Singular Value Decomposition and Least Squares Solutions," Numer. Math., **14**(5), pp. 403–420.

[15] Xu, H., Hassani, V., and Guedes Soares, C., 2019, "Uncertainty Analysis of the

Hydrodynamic Coefficients Estimation of a Nonlinear Manoeuvring Model Based on Planar Motion Mechanism Tests," Ocean Eng., **173**, pp. 450–459.

[16] Xu, H. T., Hassani, V., and Guedes Soares, C., 2018, "Parameters Estimation of Nonlinear Manoeuvring Model for Marine Surface Ship Based on PMM Tests," *ASME 2018 37th International Conference on Ocean, Offshore and Arctic Engineering*, ASME, Madrid, Spain, p. V11BT12A010.

[17] Perera, L. P., Oliveira, P., and Guedes Soares, C., 2016, "System Identification of Vessel Steering with Unstructured Uncertainties by Persistent Excitation Maneuvers," IEEE J. Ocean. Eng., **41**(3), pp. 515–528.

[18] Fossen, T. I., Sagatun, S. I., and Sørensen, A. J., 1996, "Identification of Dynamically Positioned Ships," Model. Identif. Control, **17**(2), pp. 153–165.

[19] Åström, K. J., and Källström, C. G., 1976, "Identification of Ship Steering Dynamics," Automatica, **12**(1), pp. 9–22.

[20] Luo, W. L., and Zou, Z. J., 2009, "Parametric Identification of Ship Maneuvering Models by Using Support Vector Machines," J. Sh. Res., **53**(1), pp. 19–30.

[21] Luo, W., Guedes Soares, C., and Zou, Z., 2016, "Parameter Identification of Ship Maneuvering Model Based on Support Vector Machines and Particle Swarm Optimization," J. Offshore Mech. Arct. Eng., **138**(3), p. 031101.

[22] Vapnik, V. N., 1998, *Statistical Learning Theory*.

[23] Xu, H. T., and Guedes Soares, C., 2016, "Vector Field Path Following for Surface Marine Vessel and Parameter Identification Based on LS-SVM," Ocean Eng., **113**, pp. 151–161.

[24] Xu, H. T., and Guedes Soares, C., 2016, "Waypoint-Following for a Marine Surface Ship Model Based on Vector Field Guidance Law," *Maritime Technology and Engineering 3*, C. Guedes Soares, and T.A. Santos, eds., Taylor & Francis Group, London, UK, pp. 409–418.

[25] Cauwenberghs, G., and Poggio, T., 2001, "Incremental and Decremental Support Vector Machine Learning," Adv. Neural Inf. Process. Syst., **13**(x), pp. 409–415.

[26] Guo, Z., and Guan, X., 2014, "Nonlinear Generalized Predictive Control Based on Online Least Squares Support Vector Machines," Nonlinear Dyn., **79**(2), pp. 1163–1168.

[27] Tang, H. S., Xue, S. T., Chen, R., and Sato, T., 2006, "Online Weighted LS-SVM for Hysteretic Structural System Identification," Eng. Struct., **28**(12), pp. 1728–1735.

[28] ITTC, 2002, *Recommended Procedures and Guidelines: Free Running Model Tests*.

[29] Abkowitz, M. A., 1980, "Measurement of Hydrodynamic Characteristics from Ship Maneuvering Trials by System Identification," SNAME Trans., **88**, pp. 283–318.

[30] Fossen, T. I., 2011, *Handbook of Marine Craft Hydrodynamics and Motion Control*, John Wiley & Sons, Ltd, Chichester, UK.

[31] Clarke, D., 2015, "A History of Ship Manoeuvrability Theory and Practice," *International Conference on Marine Simulation and Ship Manoeuvrability*, Newcastle upon Tyne, United Kingdom, pp. 1–27.

[32] Sutulo, S., and Guedes Soares, C., 2011, "Mathematical Models for Simulation of Manoeuvring Performance of Ships," *Maritime Engineering and Technology*, C.

Guedes Soares, Y. Garbatov, N. Fonseca, and A.P. Teixeira, eds., Taylor & Francis Group, London, pp. 661–698.

[33] Tzeng, C. Y., and Chen, J. F., 1999, "Fundamental Properties of Linear Ship Steering Dynamic Models," J. Mar. Sci. Technol., **7**(2), pp. 79–88.

[34] Suykens, J. A. K., Van Gestel, T., De Brabanter, J., De Moor, B., and Vandewalle, J., 2002, *Least Squares Support Vector Machines*.

[35] Suykens, J. A. K., and Vandewalle, J., 1999, "Least Squares Support Vector Machine Classifiers," Neural Process. Lett., **9**(3), pp. 293–300.

[36] Vapnik, V. N., 1995, "The Nature of Statistical Learning Theory," Springer, **8**(6), p. 187.

[37] Golub, G. H., and Van Loan, C. F., 2013, *Matrix Computations*.

[38] Perera, L. P., Ferrari, V., Santos, F. P., Hinostroza, M. A., and Guedes Soares, C., 2015, "Experimental Evaluations on Ship Autonomous Navigation and Collision Avoidance by Intelligent Guidance," IEEE J. Ocean. Eng., **40**(2), pp. 374–387.

[39] Hinostroza, M. A., Xu, H. T., and Guedes Soares, C., 2018, "Path-Planning and Path-Following Control System for Autonomous Surface Vessel," *Maritime Transportation and Harvesting of Sea Resources*, C. Guedes Soares, and T. A.P., eds., Taylor & Francis Group, London, UK, pp. 991–998.

[40] Clarke, D., 2003, "The Foundations of Steering and Manoeuvring," *Proceedings of the IFAC Conference on Manoeuvring and Control of Marine Craft*, IFAC, Girona, Spain.

[41] Xu, H. T., Hinostroza, M. A., and Guedes Soares, C., 2017, "A Hybrid Controller Design for Ship Autopilot Based on Free-Running Model Test," *Maritime Transportation and Harvesting of Sea Resources*, C. Guedes Soares, and A.P. Teixeir, eds., Taylor & Francis Group, London, UK, pp. 1051–1059.

[42] Journee, J. M. J., 1970, "A Simple Method for Determining the Manoeuvring Indices k and t from Zigzag Trial Data," Transl. Rep. , **267**, pp. 1–9.

Figure Captions List

Table Caption List

Figures

Fig. 1: Scaled self-running ship model in the test.

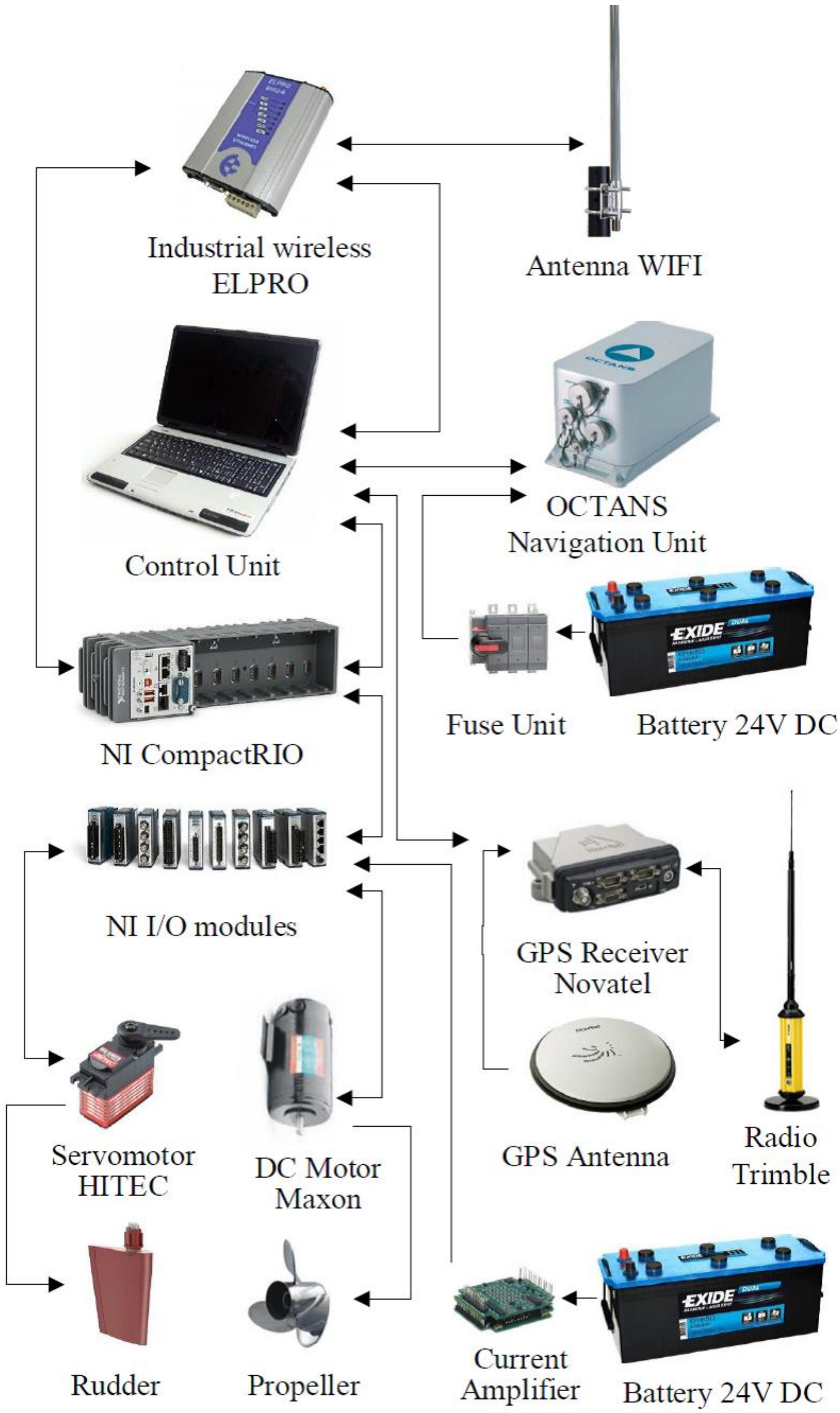

Fig. 2: Onboard sensors and actuators.

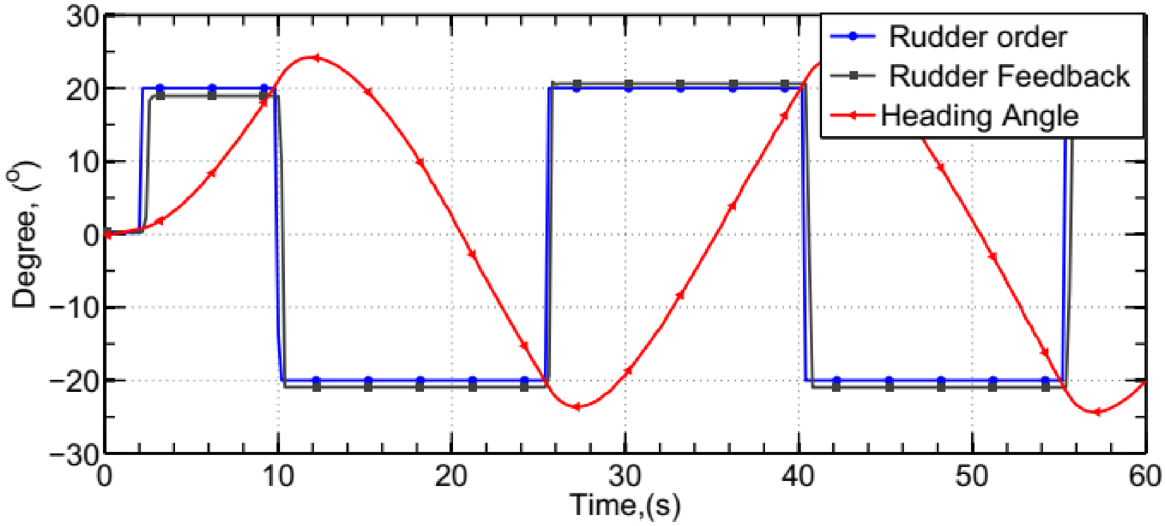

Fig 3: The $20^{\circ}-20^{\circ}$ zigzag manoeuvring test using free-running ship model.

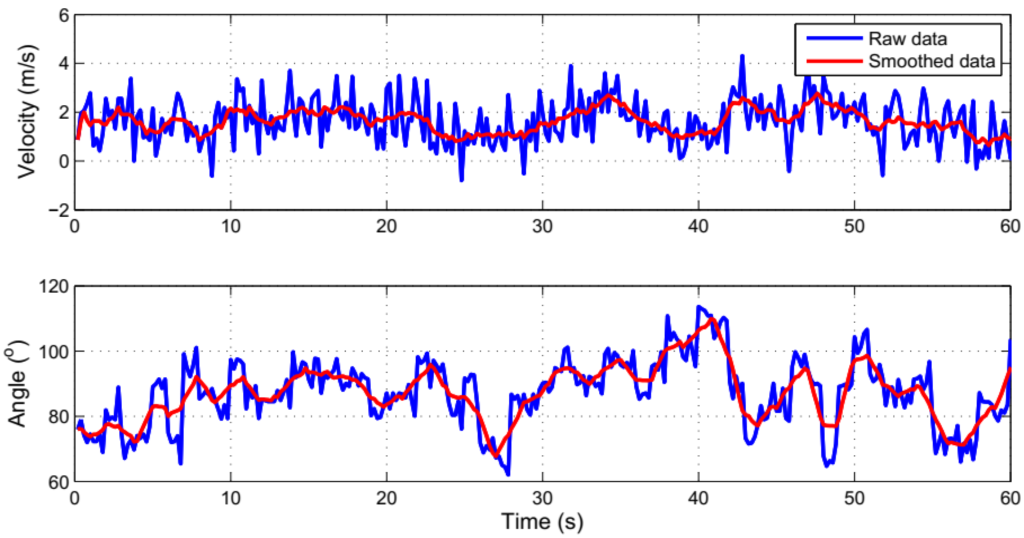

Fig 4: Wind conditions during the $20^\circ - 20^\circ$ zigzag manoeuvring tests.

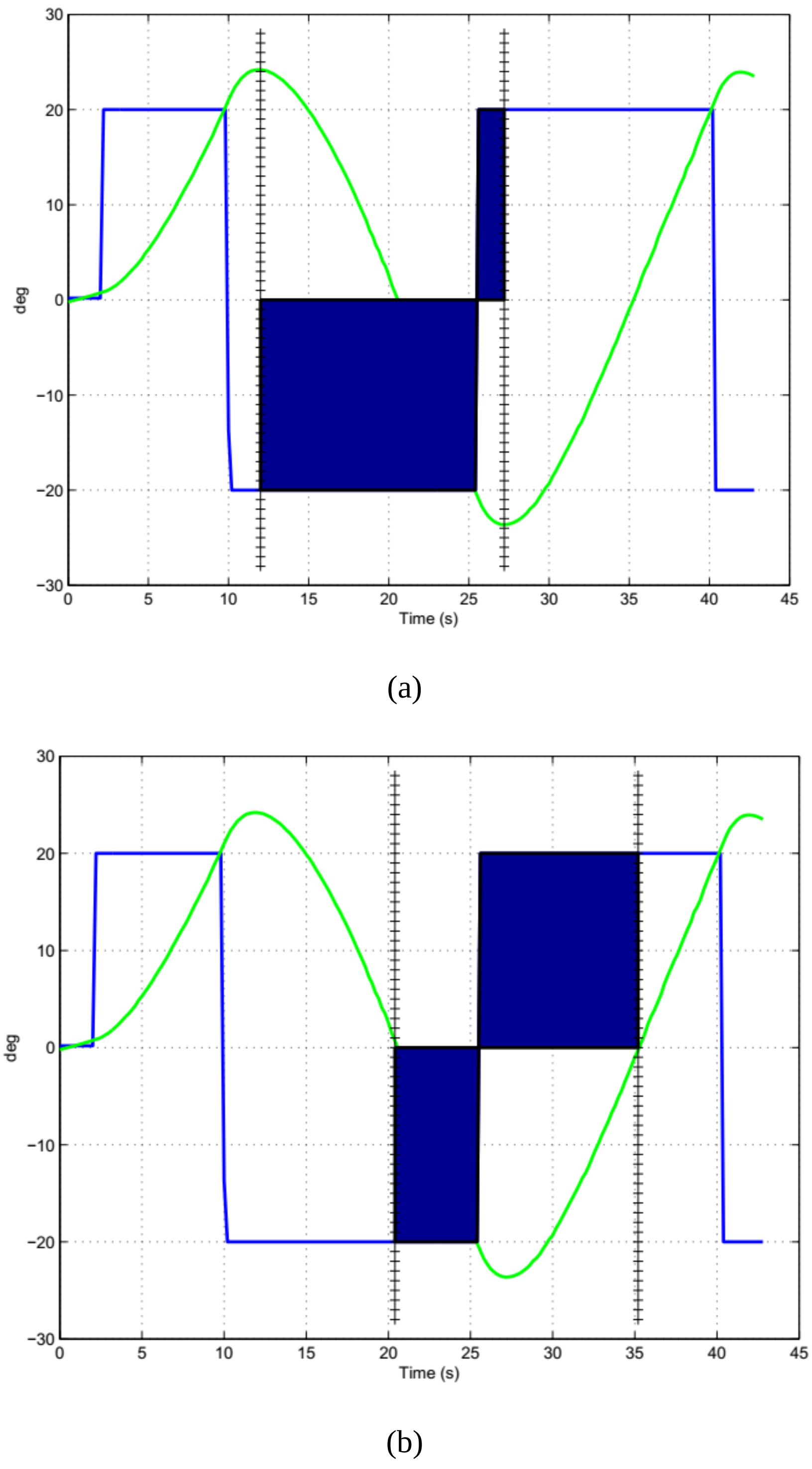

Fig. 5: Calculation of K_δ (5a) and T (5b) using $20^\circ - 20^\circ$ zigzag manoeuvring test data.

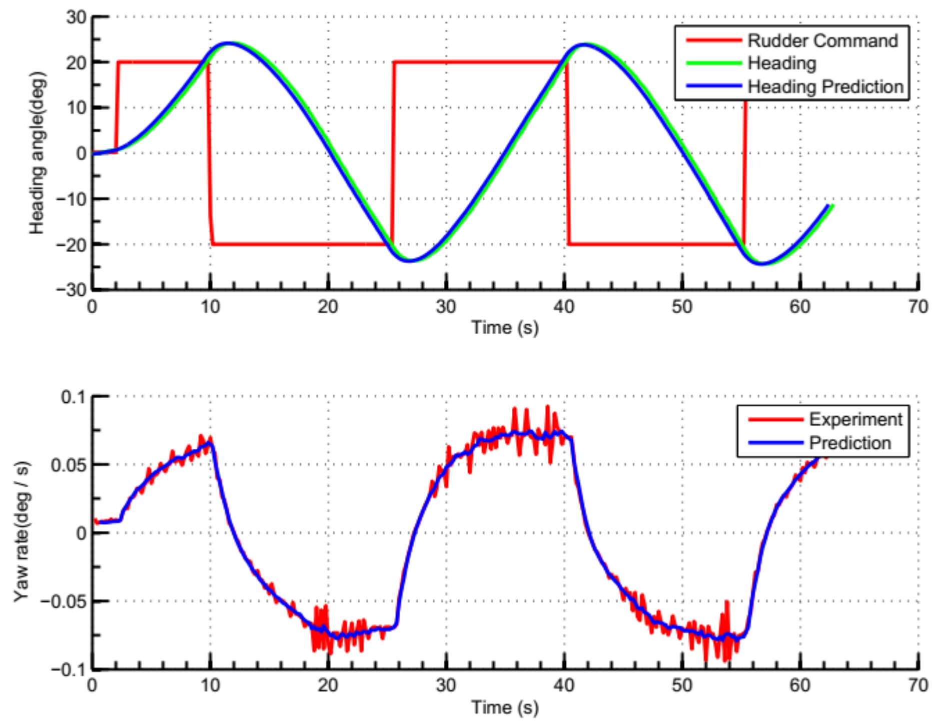

(a)

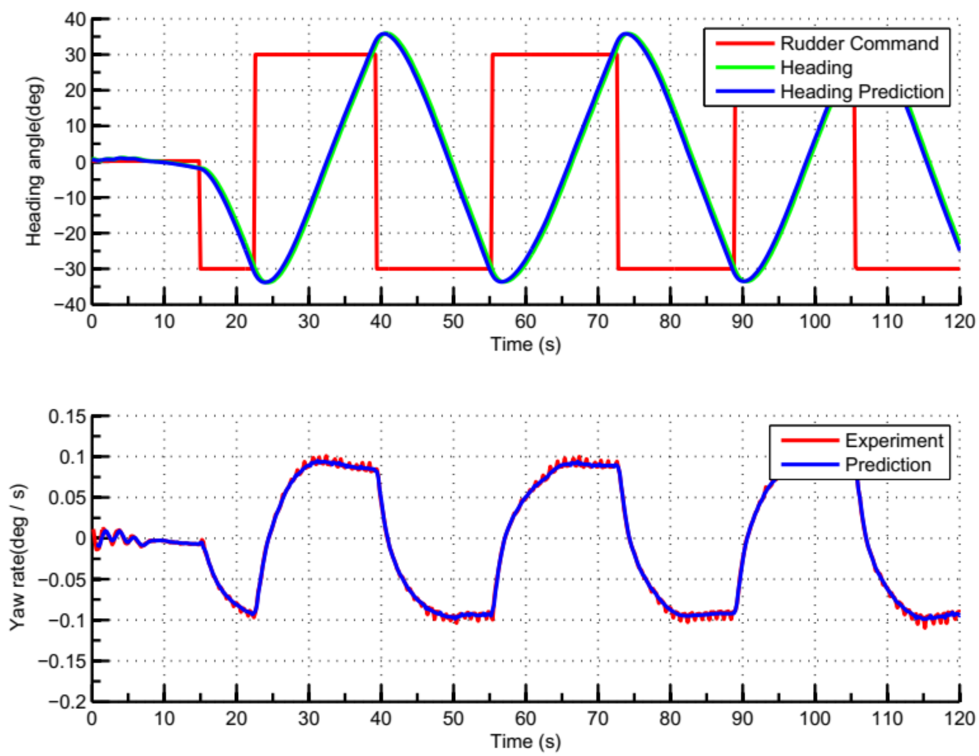

Fig 6: Prediction of $20^{\circ}-20^{\circ}$ (6a) and $30^{\circ}-30^{\circ}$ (6b) Zigzag manoeuvre using nonlinear 2nd order Nomoto model.

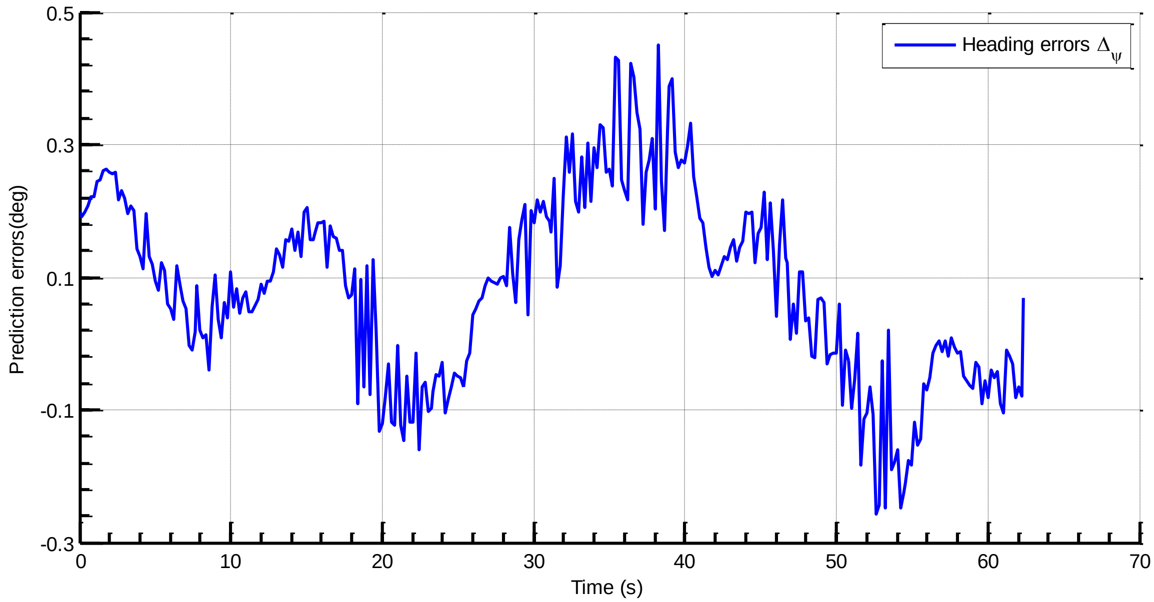

(a)

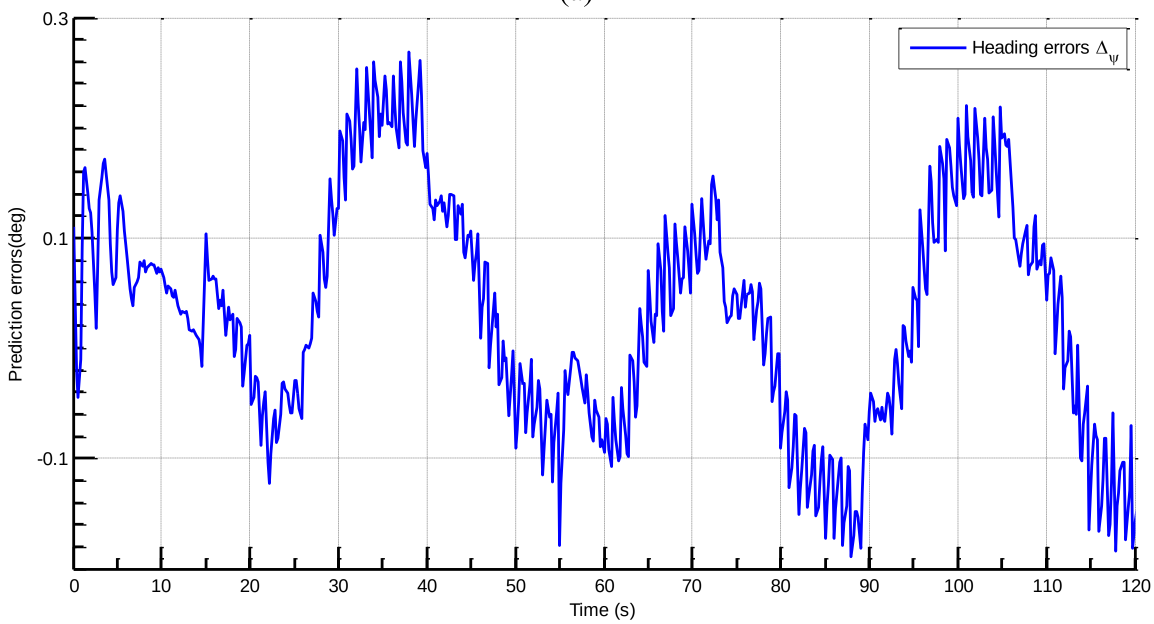

(b)

Fig 7: The heading errors of reproducing the $20^\circ - 20^\circ$ (7a) and $30^\circ - 30^\circ$ (7b) Zigzag manoeuvre using nonlinear 2nd order Nomoto model.

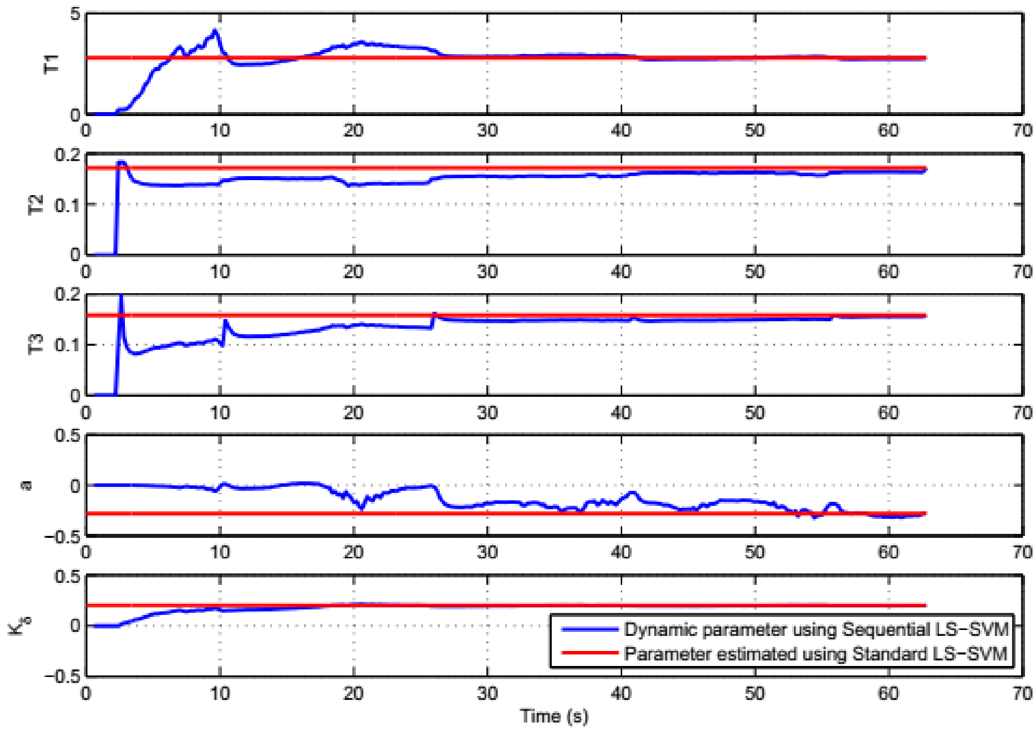

(a)

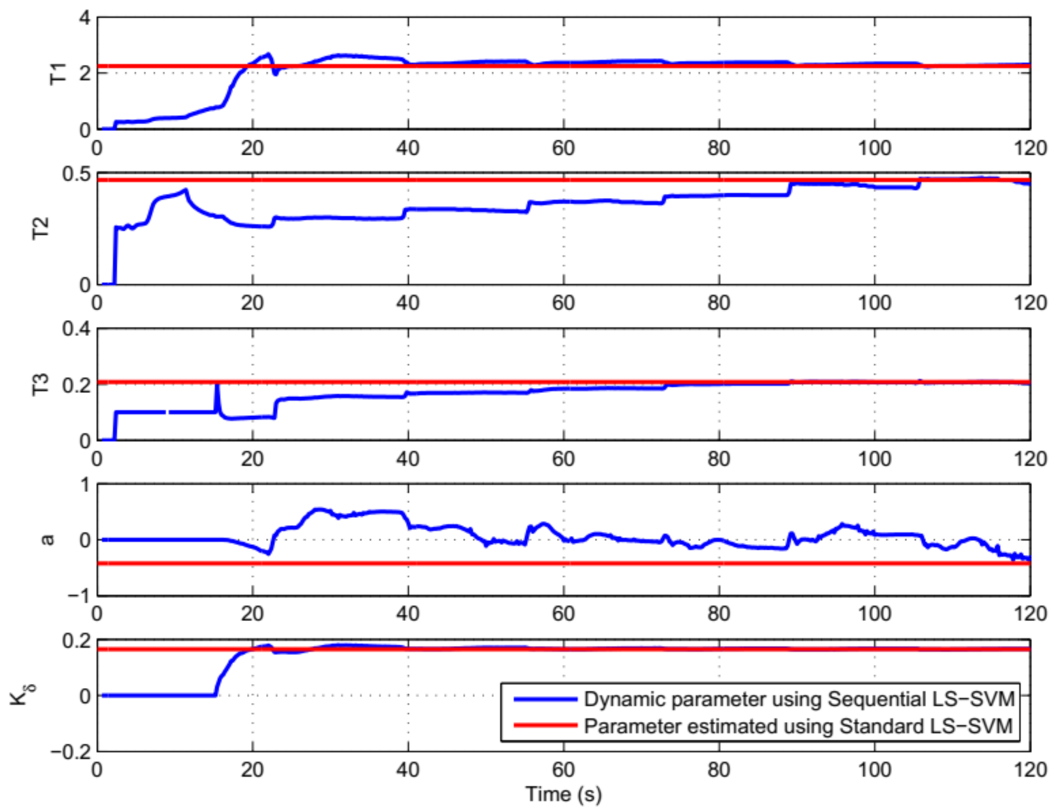

(b)

Fig 8: Real-time parameters estimation of nonlinear 2nd order Nomoto model using $20^\circ-20^\circ$ (8a) and $30^\circ-30^\circ$ (8b) Zigzag manoeuvre test data.

Tables

TABLE 1: Main particularities of the ship model

CHEMICAL TANKER MODEL	
Length (m)	2.58
Breadth (m)	0.43
Draught (estimated at the tests) (m)	0.10
Propeller diameter (m)	0.08
Design speed (m/s)	0.98
Scaling factor	

TABLE 2: The values of the parameters of 1st-order Nomoto model

Method	T	K_δ
Theoretical values	2.5221	0.2062
LS-SVM	2.8540	0.2036

TABLE 3: The parameters of Nonlinear 2nd order Nomoto Model using standard LS-SVM.

Data	T_1	T_2	T_3	a	K_δ
$20^\circ - 20^\circ$	2.7879	0.1716	0.1585	-0.2807	0.2028
$30^\circ - 30^\circ$	2.2464	0.4667	0.2082	-0.4222	0.1647

Algorithms 1: Sequential LS-SVM algorithm

Initialize:	Set $C \leftarrow 10^4; N \leftarrow 10;$
	$K(x_k \cdot x_i) \leftarrow \boldsymbol{\varphi}(x_k)^T \boldsymbol{\varphi}(x_i)$
Result:	$\boldsymbol{\theta}_{N+1}$
If	*New measurement* (x_{N+1}, y_{N+1}) **Then**
	Compute the parameter $\boldsymbol{b}$, c;
	Compute the inverse matrix $\boldsymbol{A}_{N+1}^{-1}$;
	Update the parameter matrix $\boldsymbol{\theta}_{N+1}$;
	$N \leftarrow N+1$;
else	
	Output the previous parameter $\boldsymbol{\theta}_N$
end	